Geodynamic evolution and crustal growth of the central Indian Shield: Evidence from geochemistry of gneisses and granitoids

M Faruque Hussain[1], M E A Mondal[1*] and T Ahmad[2]

[1]*Department of Geology, Aligarh Muslim University, Aligarh 202 002, India.*
[2]*Department of Geology, University of Delhi, New Delhi 110 007, India.*
[*]*e-mail: emondal@lycos.com*

The rare earth element patterns of the gneisses of Bastar and Bundelkhand are marked by LREE enrichment and HREE depletion with or without Eu anomaly. The spidergram patterns for the gneisses are characterized by marked enrichment in LILE with negative anomalies for Ba, P and Ti. The geochemical characteristics exhibited by the gneisses are generally interpreted as melts generated by partial melting of a subducting slab. The style of subduction was flat subduction, which was most common in the Archean. The rare earth patterns and the multi-element diagrams with marked enrichment in LILE and negative anomalies for Ba, P and Ti of the granitoids of both the cratons indicate interaction between slab derived melts and the mantle wedge. The subduction angle was high in the Proterozoic. Considering the age of emplacement of the gneisses and granitoids that differs by ~ 1 Ga, it can be assumed that these are linked to two independent subduction events: one during Archaean (flat subduction) that generated the precursor melts for the gneisses and the other during the Proterozoic (high angle subduction) that produced the melts for the granitoids. The high values of Mg #, Ni, Cr, Sr and low values of SiO_2 in the granitoids of Bastar and Bundelkhand cratons compared to the gneisses of both the cratons indicate melt-mantle interaction in the generation of the granitoids. The low values of Mg#, Ni, Cr, Sr and high values of SiO_2 in the gneisses in turn overrules such melt-mantle interaction.

1. Introduction

The formation and growth of continental crust have evolved through geologic time in response to gradual planetary cooling (Kröner 1985). The abundant tonalite-trondhjemite-granodiorite (TTG) suite of rocks during Archaean and its near absence during Phanerozoic is a manifestation of this evolution. The role of slab melts (whether in interaction with the mantle wedge or not) is quite significant in this evolution (Martin 1986, 1993).

In this paper we report the geochemical data of gneisses and granitoids from Bastar and Bundelkhand craton (together called central Indian Shield) and look for evidences to discern the geodynamic evolution and crustal growth of the central Indian Shield from Archaean to Proterozoic.

The available radiometric data (table 1) on Bastar (after Sarkar A *et al* 1990; Sarkar G *et al* 1990; 1993) and Bundelkhand (after Sarkar *et al* 1984; Mondal *et al* 2002) cratons reveal that the various events of felsic magmatism within the central Indian Shield are extended from mid-Archaean to Paleoproterozoic. All these events of felsic magmatism from both the cratons are grouped into two categories:

- mid-late Archaean magmatism: This episode represents the Archaean felsic magmatism within the central Indian Shield that provided

Keywords. Central Indian shield; Bundelkhand-Bastar cratons; geochemistry; gneisses; granitoids.

Proc. Indian Acad. Sci. (Earth Planet. Sci.), **113**, No. 4, December 2004, pp. 699–714
© Printed in India.

Table 1. *Geochronological data of Bastar and Bundelkhand cratons, central Indian shield.*

S. No.	Description of samples and area	Age (Ma)	Techniques used	Reference
		Bastar Craton		
1.	Orthogneiss, southern Bastar	3018 ± 61	Pb-Pb data	Sarkar A *et al* 1990
2.	Trondhjemitic gneiss, Markampara	$3509 + 14/-7$	U-Pb zircon data	Sarkar G *et al* 1993
3.	Granite, Markampara	2480 ± 3	U-Pb zircon data	Sarkar G *et al* 1993
		Bundelkhand Craton		
1.	Gneiss, Mahoba	3270 ± 3	Ion microprobe Pb-Pb zircon data	Mondal *et al* 2002
2.	Gneiss, Kuraicha	3297 ± 8	Ion microprobe Pb-Pb zircon data	Mondal *et al* 2002
3.	Gneiss, Babina	2697 ± 3	Ion microprobe Pb-Pb zircon data	Mondal *et al* 2002
4.	Gneiss, Karera	2563 ± 6	Ion microprobe Pb-Pb zircon data	Mondal *et al* 2002
5.	Hornblende Granitoid, Jakhaura	2516 ± 4	Ion microprobe Pb-Pb zircon data	Mondal *et al* 2002
6.	Biotite Granitoid, Datia	2516 ± 5	Ion microprobe Pb-Pb zircon data	Mondal *et al* 2002
7.	Leucogranitoid, Lalitpur	2492 ± 10	Ion microprobe Pb-Pb zircon data	Mondal *et al* 2002

the precursor melts for Bastar granodioritic gneisses and Bundelkhand TTG like gneisses.

- Late Archaean to Paleo-Proterozoic: This episode represents the Proterozoic felsic magmatism within the central Indian Shield, which produced the various granitoid plutons within Bundelkhand and Bastar cratons.

2. Sampling and analytical techniques

In this study we have synthesized a total of thirty samples (eighteen granitoids and twelve gneisses) from both the cratons. Out of which eleven (four gneisses and seven granitoids) samples from Bastar craton were analyzed on WD-XRF (Simens SRS 3000) at Wadia Institute of Himalayan Geology (WIHG), Dehra-Dun for major and trace elements and on ICP MS (Perkin Elmer Sciex ELAN DRC-II) at National Geophysical Laboratory (NGRI), Hyderabad for trace elements including rare earth elements. The precision of XRF major oxide data is better than 1.5% and that of the trace element data is better than 12%. Details of the analytical techniques, precision and accuracy of the machine are described by Saini *et al* (1998). The precision of the ICP MS rare earth element data is better than 5%. Details of the analytical techniques, accuracy and precision of the instrument is described by Balaram *et al* (1996). Data on rest of the samples were taken from Sarkar G *et al* (1993), Sharma and Rahman (1995) and Mondal (1995, 2001). Whole rock major and trace element data of granitoids and gneisses are presented in tables 2 and 3.

3. Geological setting

Older supracrustals, gneisses, granitoids and mafic dykes are the common litho-units that constitute the overall geology of Bastar and Bundelkhand cratons. In addition Bastar craton has a considerable thickness of unmetamorphosed younger supracrustals, which are contained within two large (Chattisgarh and Indravati) and six small Proterozoic rift related basins. Records of such younger supracrustals are missing within Bundelkhand craton possibly due to a deeper level of erosion or non-development of protracted rifting leading to the formation of basins during the Proterozoic. However there are thick sequences of metamorphosed and unmetamorphosed sedimentary sequences that are contained within Gwalior and Bijawar basins at the periphery towards north and south of Bundelkhand craton, respectively (Basu 1986).

Bastar craton is located within 17.5°N–23.5°N latitude and 77.8°E–84.1°E longitude and covers an area of approximately $2,15,000\,\mathrm{km}^2$ (figure 1). Gneisses of granitic composition are the most prominent and ubiquitous rock types of the craton

Table 2. *Whole rock geochemical analyses for the granitoids of Bastar and Bundelkhand cratons.*

	Bastar granitoids						
Major element (wt.%)	Sample no. RB 9	RB 11	RB 20	DK 21	DK 23	JT 31	BSP 101
SiO_2	72.45	75.58	72.75	65.59	73.46	71.25	70.61
TiO_2	0.17	0.08	0.23	0.40	0.11	0.36	0.13
Al_2O_3	13.97	12.5	12.94	12.5	13.37	15.30	15.91
$Fe_2O_3^{(T)}$	1.82	1.58	2.48	4.21	1.78	2.55	1.71
MnO	0.02	0.01	0.03	0.14	0.03	0.02	0.02
MgO	0.34	0.31	0.49	1.41	0.38	0.55	0.22
CaO	1.47	0.65	3.6	5.98	0.72	0.84	2.20
Na_2O	4.18	3.21	4.17	3.02	3.67	2.28	3.80
K_2O	4.01	5.43	1.95	3.99	4.98	3.38	6.80
P_2O_5	0.05	0.01	0.07	0.38	0.03	0.01	0.01
LOI	1.02	0.37	1.06	1.53	1.32	1.97	0.03
Total	99.5	99.73	99.77	99.15	99.85	98.51	101.44
Mg#	19.63	20.42	20.53	30.35	21.82	22	14.47
	Trace elements in ppm						
Cu	16	4	2	11	17	14	2
Ni	10	16	10	54	18	44	6
Co	nd	69	3	57	nd	nd	2
Sc	1	18	5	7	2	4	11
Zn	25	34	37	83	23	46	26
Ga	19	17	16	16	19	20	18
Pb	45	112	16	25	38	34	59
Cr	295	93	350	45	352	600	195
Th	11	72	16	16	60	43	86
Rb	124	348	44	117	284	183	263
U	6	22	1.5	3	13	8	8
Sr	269	47	410	813	86	239	271
Y	6	94	23	35	30	30	64
Zr	158	497	313	337	124	383	477
Nb	6	23	8	33	23	18	18
Ba	1216	79	732	570	259	1009	399
V	nd	2.5	18	nd	nd	nd	23
Hf	nd	nd	nd	nd	nd	nd	nd
Ta	nd	nd	nd	nd	nd	nd	nd
La	nd	47.8	52.5	63.2	nd	nd	64
Ce	nd	110	109.2	172	nd	nd	145
Pr	nd	13.8	13.3	26	nd	nd	18
Nd	nd	41.7	40.2	88	nd	nd	54
Sm	nd	8.5	6.2	12.6	nd	nd	10
Eu	nd	2.1	1.2	2.2	nd	nd	0.6
Gd	nd	7.1	4.5	8.9	nd	nd	7.8
Tb	nd	1.6	0.7	1.3	nd	nd	1.6
Dy	nd	9.1	3.2	5.3	nd	nd	8.3
Ho	nd	1.8	0.6	0.9	nd	nd	1.6
Er	nd	6.3	1.9	2.9	nd	nd	4.8
Tm	nd	1.1	0.3	0.4	nd	nd	0.8
Yb	nd	7.5	2	2.9	nd	nd	5
Lu	nd	1.2	0.3	0.5	nd	nd	0.8

Table 2. *(Continued)*

	Bundelkhand Granitoids (data are after Mondal 1995)							
Major element (wt.%)	Sample no. 41 C	46	115	121	126	219	244	38 A
SiO_2	59.46	48.99	58.01	49.03	54.98	51.54	62.05	71.01
TiO_2	0.73	1.24	1.25	0.91	0.52	0.52	0.57	0.37
Al_2O_3	15.91	17.12	18.26	17.45	12.75	14.91	16.56	13.79
$Fe_2O_3^{(T)}$	6.51	9.53	7.18	8.86	8.05	10.95	5.59	2.59
MnO	0.11	0.14	0.15	0.13	0.16	0.17	0.08	0.04
MgO	4.28	6.08	2.3	7.2	6.99	6.93	2.96	0.45
CaO	4.79	9.20	7.36	8.3	7.47	10	4.04	1.45
Na_2O	2.71	2.31	2.72	2.97	2.20	2.69	3.24	3.39
K_2O	3.62	1.45	1.34	2.45	2.97	0.3	4.14	5.29
P_2O_5	0.91	0.48	0.66	0.33	0.37	0.74	0.35	0.05
LOI	0.79	1.75	1.21	1.68	1.78	1.33	0.96	0.78
Total	99.82	98.29	100.44	99.31	98.24	100.08	100.54	99.21
Mg#	46.22	45.48	29.52	51.52	53.17	45.28	40.91	18.45
	Trace elements in ppm							
Cu	7	13	26	120	102	481	197	8
Ni	14	21	51	nd	nd	157	78	12
Co	51	34	52	nd	nd	76	31	42
Sc	10	15	20	nd	nd	18	14	9
Zn	53	88	50	203	117	nd	nd	67
Ga	22	23	14	19	19	20	23	21
Pb	2	2	4	nd	4	nd	nd	5
Cr	25	18	160	nd	nd	26	140	32
Th	11	2	1	13	11	1	16.77	16
Rb	99	37	9	75	134	10	214	117
U	2	0.3	0.3	nd	12	0.2	5	3
Sr	452	1113	171	901	352	579	388	398
Y	32	15	11	2	22	7	30	33
Zr	175	36	27	68	133	27	257	195
Nb	13	3	2	nd	8	3	21	13
Ba	389	239	35	nd	nd	155	2497	526
V	75	142	114	nd	nd	472	227	72
Hf	16	4	4	nd	nd	1	6	23
Ta	3	1	4	nd	nd	1	2	15
La	28	13	3	nd	nd	10	93	29
Ce	84	36	9	nd	nd	15	119	82
Pr	nd	nd	nd	nd	nd	nd	nd	nd
Nd	30	17	4	nd	nd	10	50	32
Sm	3	2	1	nd	nd	2	7	5
Eu	0.5	0.7	0.2	nd	nd	0.9	2	0.7
Gd	2	1.8	0.7	nd	nd	2	7	3
Tb	nd	nd	nd	nd	nd	nd	nd	nd
Dy	3	2	1.5	nd	nd	1.6	6	4
Ho	nd	nd	nd	nd	nd	nd	nd	nd
Er	nd	nd	nd	nd	nd	nd	nd	nd
Tm	nd	nd	nd	nd	nd	nd	nd	nd
Yb	2	1	1	nd	nd	1	3	3
Lu	nd	nd	nd	nd	nd	nd	nd	nd

Table 2. *(Continued)*

	Bundelkhand Granitoids (data are after Mondal 1995)		
Major element (wt.%)	Sample no. 123	206	234
SiO_2	63.56	71.32	72.67
TiO_2	0.55	0.21	0.18
Al_2O_3	16.13	14.25	13.69
$Fe_2O_3^{(T)}$	4.96	1.92	1.72
MnO	0.09	0.03	0.03
MgO	1.53	0.47	0.23
CaO	4.26	0.66	0.99
Na_2O	3.78	3.06	3.39
K_2O	3.95	5.33	4.92
P_2O_5	0.31	0.04	0.02
LOI	0.68	0.97	0.81
Total	99.8	98.26	98.65
Mg#	28.34	24.25	14.88
	Trace elements in ppm		
Cu	6	193	234
Ni	12	47	47
Co	17	40	32
Sc	9	8	5
Zn	103	nd	nd
Ga	23	29	27
Pb	5	nd	nd
Cr	12	17	15
Th	5	24	36
Rb	47	292	285
U	1	5	5
Sr	872	119	88
Y	18	23	29
Zr	41	190	182
Nb	6	17	17
Ba	368	727	541
V	62	116	206
Hf	6	5	5
Ta	2	3	3
La	23	61	87
Ce	67	126	151
Pr	nd	nd	nd
Nd	28	42	60
Sm	4	9	12
Eu	1	1	1
Gd	2	7	9
Tb	nd	nd	nd
Dy	3	4	6
Ho	nd	nd	nd
Er	nd	nd	nd
Tm	nd	nd	nd
Yb	2	2	3
Lu	nd	nd	nd

LOI: loss of ignition.
nd: not determined

that form the basement for the older supracrustals (consisting of quartzites, phyllites, mica schists, banded hematite quartzites and agglomerates) especially in the north, northwest and southern part of the craton. Besides forming large outcrops, the gneisses also occur as enclaves within the granitoids of younger magmatic activities. The gneisses which form the basement of Bastar craton yielded a whole rock Rb-Sr and Pb-Pb isochron age of $\sim$ 3.0 Ga (Sarkar G *et al* 1990; Sarkar A *et al* 1990). However, one gneissic sample of TTG like characteristics occurring as enclave within granitoid in Bastar craton has yielded Pb-Pb zircon age of $\sim$ 3.5 Ga (Sarkar G *et al* 1993). We have made detailed field investigations in Bastar craton but have not observed any evidence like cross-cutting or intrusive relationship of one gneiss into the other to suggest two distinct generations of gneisses. Besides, on the basis of geochemical data, it has also been observed that the gneisses are cogenetic and comagmatic and the differences in their age are mainly due to different chronometers used for dating the gneisses (Hussain *et al* 2004).

The Bundelkhand craton lies approximately between 24°30′N and 26°N latitude and 27°30′E and 81°E longitude and occupies an area of about 26,000 km^2 (figure 1). The gneisses of Bundelkhand craton are trondhjemitic in nature, which intrude into the older supracrustals consisting of amphibolites, quartzites, banded magnetite quartzites and schists. The gneisses are gray to pink, medium to fine grained with occasional porphyroblasts of feldspars (Sharma and Rahman 1995). The Bundelkhand gneisses are prominently exposed along two linear belts of about one kilometer long and 500 m wide along Mahoba-Charkari and Mahoba-Kabrai roads and along Kabrai to Karera through Kuraicha. Enclaves of these gneisses also occur abundantly within the granitoids of later magmatic events. The precursor magmatism of Bundelkhand basement gneisses took place at $\sim$ 3.3 Ga (Pb-Pb zircon age data, Mondal *et al* 2002).

The granitoids of Bundelkhand massif are the most voluminous rock suites of batholithic dimensions. The granitoids have intruded into the older supracrustals (consisting of BIF, metasediments, mafic and ultramafic rocks) and into the gneisses. The granitoids are almost undeformed and contain xenolithic enclaves of older supracrustals and gneisses. They are generally coarse to medium grained and occasionally contain phenocrysts of K-feldspars. The granitoid magmatism within the Bundelkhand massif was followed by large-scale mafic dyke emplacement events. Emplacement of mafic-ultramafic bodies, rhyolites, pegmatites and quartz veins followed the dyking events. The Pb-Pb zircon age of the Bundelkhand granitoids (Mondal *et al* 2002) suggests that the emplacement age of

Table 3. *Whole rock geochemical analyses for the gneisses of Bastar and Bundelkhand cratons.*

	Bundelkhand gneisses (data are after Sharma and Rahman 1995)					Bastar Gneisses (data are after Sarkar G *et al* 1993)		
Major element (wt.%)	Sample no. G-21	G-22	G-24	G-25	G-27	Sample no. 55	60	63
SiO_2	70.69	70.01	69.94	69.45	69.96	69.27	68.70	69.01
TiO_2	0.27	0.27	0.28	0.27	0.27	0.35	0.43	0.45
Al_2O_3	15.89	16.02	16.21	16.49	16.02	14.67	15.81	15.59
$Fe_2O_3^{(T)}$	1.55	1.58	1.77	1.77	1.61	2.87	3.59	3.54
MnO	0.04	0.03	0.04	0.06	0.05	0.02	0.03	0.03
MgO	0.81	0.82	0.77	0.72	0.66	0.54	0.67	0.71
CaO	1.83	2.17	1.97	2.06	2.17	3.45	2.45	2.72
Na_2O	5.62	5.67	5.87	6.08	5.55	3.97	4.38	4.43
K_2O	2.71	2.71	2.46	2.51	2.75	2.78	2.79	2.26
P_2O_5	0.1	0.12	0.11	0.11	0.12	0.11	0.13	0.12
Total	99.51	99.4	99.42	99.52	99.16	98.03	98.98	98.86
Mg#	40.59	40.43	36.26	34.72	34.89	19.74	19.57	20.78
Trace elements in ppm								
Cu	NA	4	10	14	10	NA	NA	NA
Ni	2	1	1			NA	NA	NA
Co	NA	NA	NA	NA	NA	NA	NA	NA
Sc	1.4	1.5	2	2	2	NA	NA	NA
Zn	43	66	49	44	51	NA	NA	NA
Ga	19	18	20	19	18	NA	NA	NA
Pb	NA	NA	NA	NA	NA	NA	NA	NA
Cr	11	21	12	9	18	NA	NA	NA
Th	25	17	21	21	4	NA	NA	NA
Rb	107	86	117	195	153	NA	NA	NA
U	9	6	6	6	4	NA	NA	NA
Sr	647	910	722	759	653	NA	NA	NA
Y	10	13	10	10	11	NA	NA	NA
Zr	171	160	199	190	180	NA	NA	NA
Nb	14	10	13	11	10	NA	NA	NA
Ba	657	643	581	562	709	NA	NA	NA
V	15	15	15	14	13	NA	NA	NA
La	52	NA	59	NA	NA	67	85	78
Ce	81	NA	87	NA	NA	104	133	117
Pr	NA	NA	NA	NA	NA	10	13	11.9
Nd	29	NA	33	NA	NA	35	48	42
Sm	5.2	NA	6	NA	NA	6.12	8.64	7.8
Eu	1.1	NA	1.2	NA	NA	1.16	1.23	1.15
Gd	3	NA	3.4	NA	NA	13.8	4.8	4.5
Tb	NA	NA	NA	NA	NA	0.41	0.52	0.48
Dy	1.9	NA	2	NA	NA	1.83	2.01	2.2
Ho	NA	NA	NA	NA	NA	0.34	0.39	0.45
Er	0.9	NA	0.9	NA	NA	0.98	0.89	0.94
Tm	NA	NA	NA	NA	NA	0.11	0.12	0.12
Yb	0.8	NA	0.8	NA	NA	0.74	0.64	0.62
Lu	0.11	NA	0.12	NA	NA	0.12	0.08	0.08

Table 3. *(Continued)*

	Bastar Gneisses			
Major element (wt.%)	Sample no. RB 13	RB 15	DK 29	GD 42
SiO_2	74.59	70.13	69.92	70.19
TiO_2	0.15	0.27	0.16	0.23
Al_2O_3	13.15	15.25	14.49	14.45
$Fe_2O_3^{(T)}$	1.72	2.99	2.09	1.99
MnO	0.02	0.03	0.03	0.02
MgO	0.34	0.66	0.47	0.59
CaO	1.38	2.44	1.75	2.09
Na_2O	3.39	4.62	5.62	4.83
K_2O	4.32	2.73	1.32	2.02
P_2O_5	0.03	0.08	0.02	0.03
Total	99.09	99.2	95.87	96.44
Mg#	20.54	22.34	22.64	27.94
	Trace elements in ppm			
Cu	1	2	2	1
Ni	11	8	12	9
Co	51	5	44	34
Sc	2	4	6	3
Zn	29	42	45	47
Ga	14	18	24	18
Pb	27	96	28	28
Cr	13	288	12	7
Th	8	13	19	46
Rb	109	88	92	62
U	2	4	13	2
Sr	225	367	209	379
Y	13	20	31	14
Zr	179	351	310	427
Nb	9	10	27	10
Ba	1122	947	75	547
V	7	16	6	8
La	12.5	28.3	23.5	55
Ce	27.5	58.6	51.5	108
Pr	3.6	7	6.4	13
Nd	11.3	21.2	19.9	38
Sm	2.6	3.8	4.4	6.4
Eu	1.1	1	0.4	0.8
Gd	1.8	2.9	3.6	4.9
Tb	0.3	0.5	0.7	0.7
Dy	1.8	2.6	3.5	2.6
Ho	0.3	0.5	0.7	0.4
Er	1	1.5	2.1	1
Tm	0.2	0.3	0.4	0.1
Yb	1.1	1.8	2.4	0.8
Lu	0.2	0.3	0.4	0.1

NA: Not analysed.

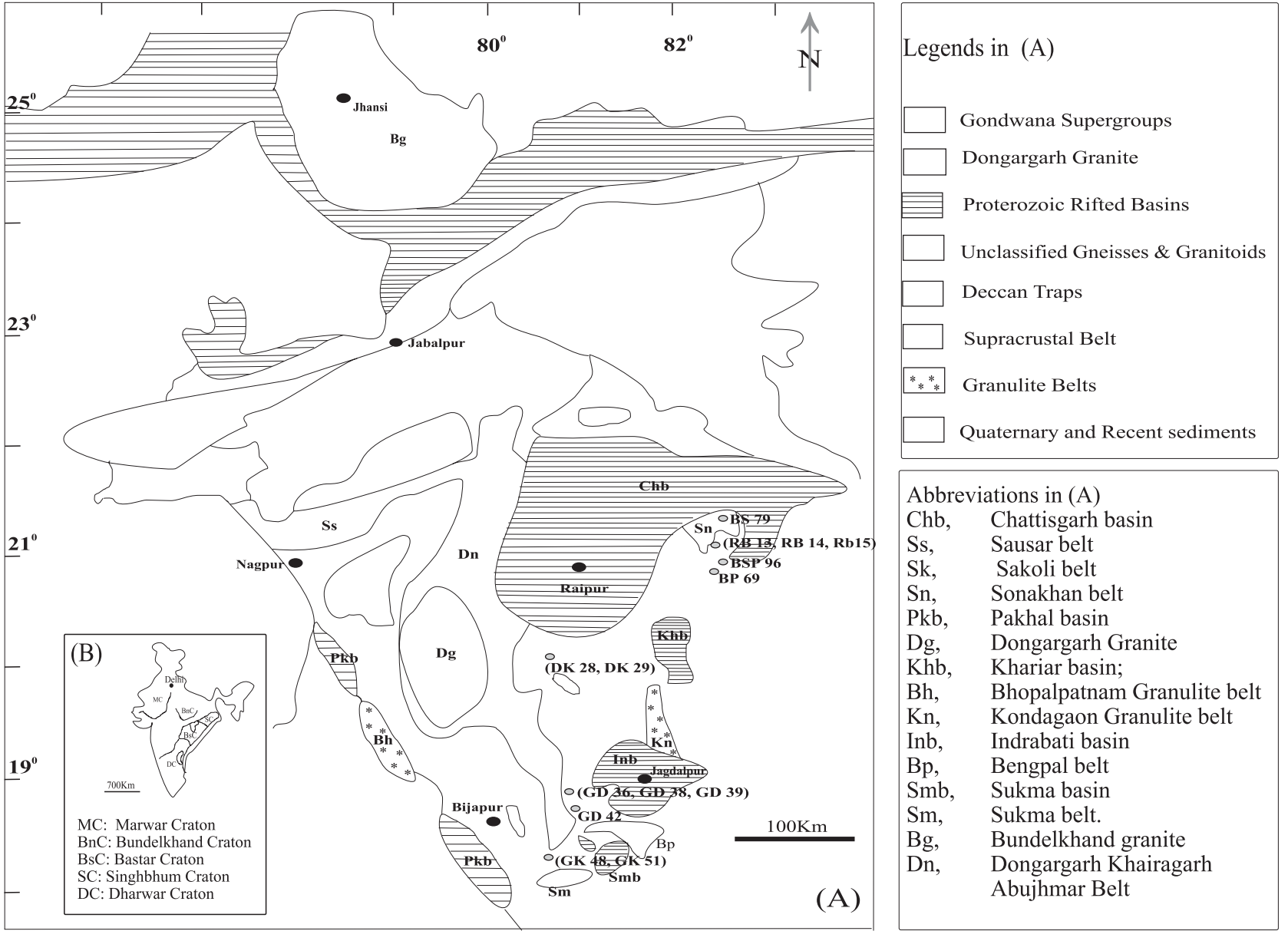

Figure 1. Simplified geological map of central Indian Shield (after Acharyya and Roy 2000). **Inset:** Geological map of India showing major Archaean cratons including Bastar and Bundelkhand (modified after Radhakrishna and Naqvi 1986).

the granitoids is ~ 2.5 Ga. Thus, it appears that the felsic magmatism of Bundelkhand craton is almost synchronous with the late Archaean felsic magmatism of Bastar craton.

4. Geochemical characteristics

4.1 *Gneisses*

The Bundelkhand gneisses have a restricted range of SiO_2 (69.45–70.69 wt.%), Al_2O_3 (15.89–16.49 wt.%), MgO (0.66–0.82 wt.%) CaO (1.83–2.17 wt.%) Na_2O (5.55–6.08 wt.%) and K_2O (2.46–2.75 wt.%) (Sharma and Rahman 1995, 1996). The gneisses are poor in ferromagnesian components ($Fe_2O_3^T + MgO + TiO_2 < 5$ wt.%). The gneisses have low Y (10–13 ppm), Cr (9–21 ppm) Nb (10–14 ppm) and high Sr contents (average 772 ppm) similar to Archaean high Al-TTG rocks reported from different cratons around the globe (Sharma and Rahman 1995, 1996).

The gneisses of Bastar craton are highly siliceous ($69.92 \leq SiO_2 \leq 74.59$ wt.%) averaging 71.21 wt.%. The Al_2O_3 concentration ($13.15 \leq Al_2O_3 \leq 15.15$ wt.%) averages 14.34 wt.%. For most of the rock samples the Al_2O_3 contents are < 15 wt.% at SiO_2 value of ≥ 70 wt.%; which is a characteristic feature of the low alumina trondhjemites (Barker and Arth 1976). The molar alumina saturation index (A/CNK) values of the Bastar gneisses ranges from 1.02 to 1.21 and the gneisses can be categorized as peraluminous. The gneisses are poor in ferromagnesian components ($Fe_2O_3 + MgO + TiO_2 = 3.19$ wt.%) and have low Mg# [$100 \times Mg^{2+}/(Mg^{2+} + Fe^{2+})$] values averaging 21.

4.2 *Granitoids*

The granitoids of Bundelkhand massif have a large variation in SiO_2 contents ranging from 49.03 to 72.67 wt.%. The granitoids have very high Al_2O_3 contents ranging from 13.69 to 18.26 wt.%. The total iron contents of the granitoids are also very high reaching up to 9.53 wt.%. Na_2O and K_2O content of the Bundelkhand granitoids averages around 3 wt.% each. The granitoids have high Cr and Ni contents ranging from 12 to 160 ppm and 12 to 157 ppm, respectively. All the granitoids are metaluminous to peraluminous in nature with molar A/CNK values ranging from 0.45 to 1.36.

The granitoids of Bastar craton have SiO_2 values ranging from 65.59 wt.% to 75.58 wt.%. The Al_2O_3 content of the Bastar granitoids ($12.45 \leq Al_2O_3 \leq 16.01$ wt.%) averages 14.25 wt.% and show peraluminous nature with the molar A/CNK values ranging from 1.16 to 1.35. Bastar granitoids have a relatively higher ferromagnesian content ($Fe_2O_3^T + MgO + TiO_2$ ranging from 1.27 to 6.02 wt.%) and accordingly have relatively higher Mg# averaging 45 compared to the gneisses with average Mg# value of 21. The K/Rb values of the granitoids ranges from 130 to 368, which are broadly comparable to the commonly occurring calc-alkaline suites (e.g. Bertrand *et al* 1984). The values for Zr/Hf (26–52), Rb/Sr (< 1), Rb/Zr (0.2–2.3) and Nb/Ta (1–13) of the Bastar granitoids are in the range of plutonic rocks found in continental magmatic arc (after Ayuso and Arth 1992). Almost all the granitoids have high K_2O values compared to the Na_2O values with K_2O/Na_2O ratio averaging 1.2. This marks a secular change in the increase of K_2O content and a simultaneous decrease of the Na_2O content from Archaean to Proterozoic.

All the major elements of the gneisses and granitoids when plotted against SiO_2 on Harker's variation diagram (not shown here), exhibit overall negative trends against SiO_2 except K_2O which shows positive correlation. Although the plots show overall negative trends, the data exhibit considerable scattering. This may indicate the presence of some sort of chemical heterogeneity (sub-groups) within larger chemical groupings and it may partly be due to alteration effects.

5. Petrogenesis

The gneisses of both the cratons of central Indian Shield are characterized by highly fractionated REE patterns ($La_N/Yb_N = 43$–50 for Bundelkhand and 8–51 for Bastar craton) with concave upward shape at HREE ends without any significant Eu anomaly (figure 2a). The REE patterns of the granitoids show flat trends with strong to insignificant Eu anomalies (figure 2b). The patterns observed in gneisses are similar to the typical high Al-TTG suites reported from different Archaean cratons around the world. Such fractionated elemental patterns are generally interpreted by partial melting of metamorphosed hydrated basalt, most likely in a subduction environment. The strongly fractionated REE patterns and HREE depletion suggest that hornblende and/or garnet may be the residual phase in the source. Heavy-REE (Dy – Lu) and Y are highly compatible in garnet and medium- to heavy-REE (Gd – Lu) and Y are compatible in amphibole. Such depleted patterns of middle- and heavy-REE, thus point to their retention by amphibole and garnet at the site of partial melting. The plots of the gneisses from both the cratons on the Sr/Y vs. Y diagram suggest that the precursor melts for the gneisses were generated by partial melting of a source rock comprising 10% garnet amphibolite restite (Drummond and Defant

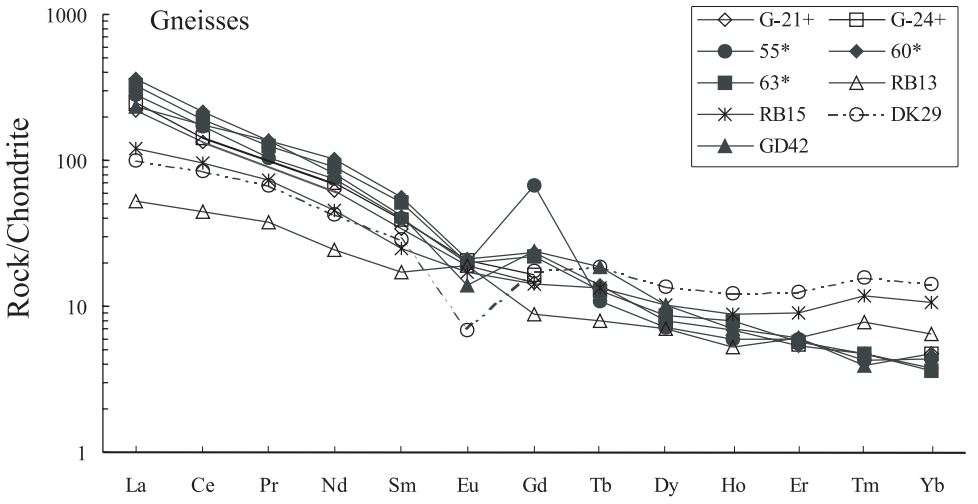

Figure 2**(a)**. Chondrite normalized rare earth element patterns for the gneisses of Bastar and Bundelkhand cratons. Normalizing values are from Sun and McDonough (1989).

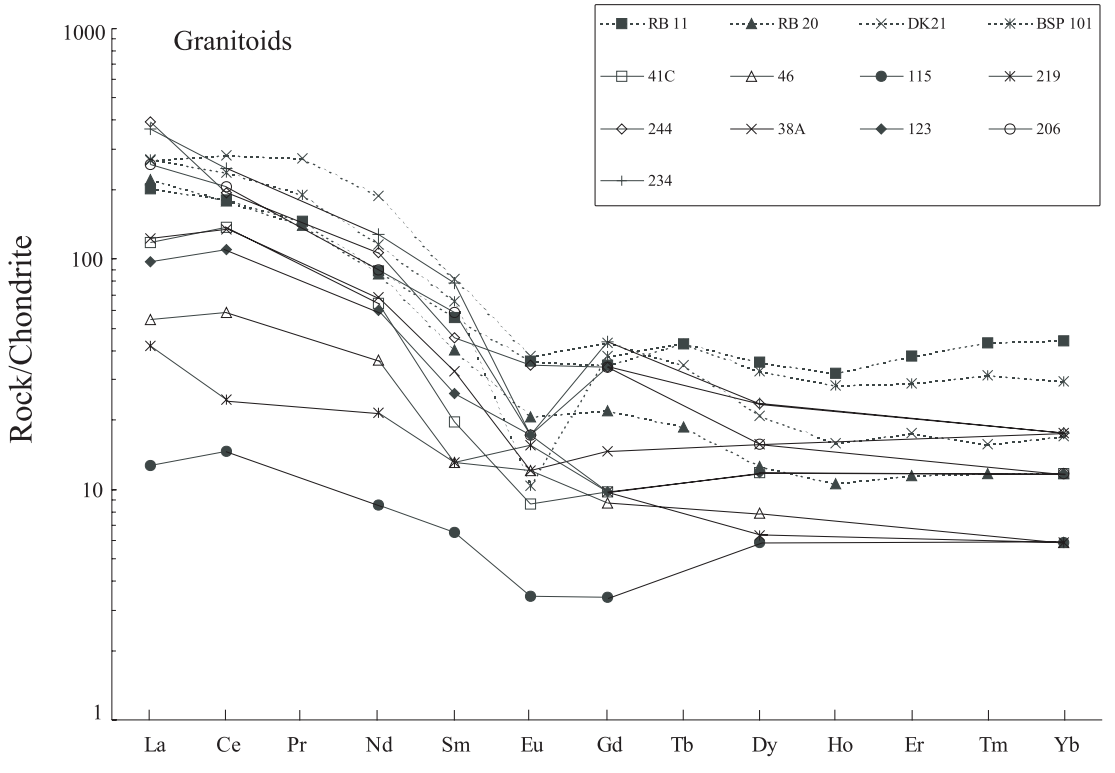

Figure 2**(b)**. Chondrite normalized rare earth element patterns for the granitoids of Bastar and Bundelkhand cratons. Normalizing values are from Sun and McDonough (1989).

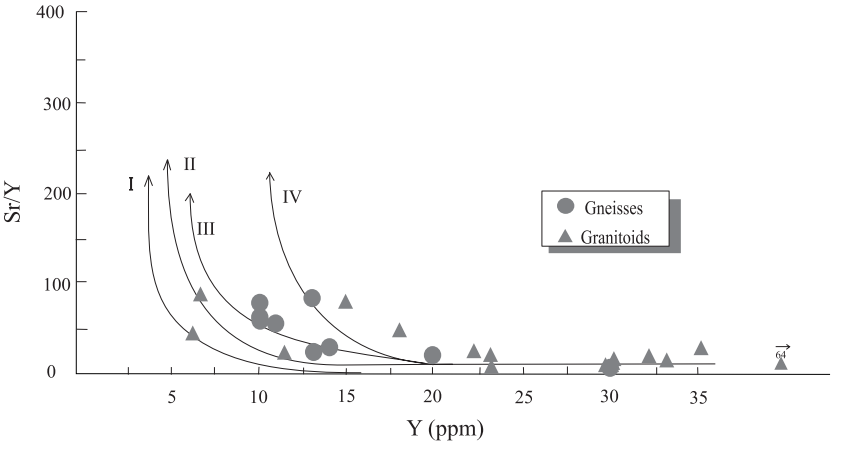

Figure 3. Y vs. Sr/Y diagram for the gneisses and granitoids of Bastar and Bumdelkhand cratons. Curves are after Drummond and Defant (1990). I and III are partial melting curves of an average mid-oceanic ridge basalt (MORB) and an Archaean mafic composite (AMC) leaving an eclogite restite. II and IV are partial melting curves of MORB and the AMC leaving a 10% garnet amphibolite restite.

1990) (figure 3). Since Y is compatible in garnet and hornblende, the presence of garnet and amphibole in the residue, thus will deplete Y contents in the melt. Furthermore, plagioclase contains Sr (and Eu) and any melt produced in the absence of residual plagioclase will be enriched in Sr contents. Since melting of wet basalt at high P_{H_2O} destabilizes plagioclase and stabilizes garnet (Garrison and Davidson 2003), high Sr/Y ratio implies partial melting of a basaltic source (eclogite, amphibolite or garnet-amphibolite) in a high P_{H_2O} environment where garnet is stable but plagioclase is not stable. This corresponds to a subduction zone environment. The primordial mantle normalized multi-elemental patterns of the gneisses from the Bundelkhand and Bastar cratons show marked enrichment in the LILE simultaneously with a lesser abundance of HFSE and strong negative anomalies at Ba, P and Ti (figure 4a). The spidergram of the granitoids from both the cratons also exhibit the similar patterns with LILE (especially Rb, Ba, Th, U and K) enrichment compared to HFSE (figure 4b). Among the HFSE, Ti is strongly depleted and P and Nb relatively weakly depleted with respect to the neighbouring elements (figure 4b). Such multi-elemental patterns are typical of subduction zone magmatism (Peacock 1990; Saunders *et al* 1991; Hawkesworth 1994). It is proposed that due to very high geothermal gradient during Archaean, the subducted slab did not dehydrate, but it got melted, leaving some refractory residue. The role of refractory phases like apatite, rutile, titanite, ilmanite becomes significant as they contain the HFSE especially P and Ti and hence their presence in the residue will deplete the melt in the HFSE and yield a corresponding enrichment of the LILE.

The signatures of subduction zone magmatism were further revealed in the tectonic discrimination diagrams especially in the Rb vs. (Y + Nb) and Nb vs. Y diagram of Pearce *et al* (1984) (figure 5). Majority of the samples of the gneisses and granitoids of Bastar and Bundelkhand cratons plot within the volcanic arc granite field. However, a few samples plot on the within-plate field. Therefore, on the basis of the above observations exhibited by the Archaean gneisses and Proterozoic granitoids from both the cratons, it is proposed that the Archaean and Proterozoic felsic magmatic rock suites from both the terrains were emplaced in temporally separate subduction zone environments in the Archaean and Proterozoic, respectively. However, as subduction ceased, both the cratonic blocks experienced lithospheric extension and rifting during Proterozoic resulting in rift related within plate felsic magmatism and mafic magmatism in the form of mafic dykes and dyke swarms. These rifts later widened and sedimentation started in the Bastar craton. This inference is corroborated by occurrences of inter-layered sedimentary rocks varying in composition from immature arkose to the mature orthoquartzites (Neogi *et al* 1996) in the Bastar craton. The rifting/extensional regime in the Bundelkhand region was not protracted and as a result no such rifted basins were developed in the Bundelkhand craton (Mondal and Ahmad 2001).

6. Tectonic setting

It is generally agreed that the Archaean gneisses of TTG characteristics are generated by partial melting of hydrated basalt in a subduction

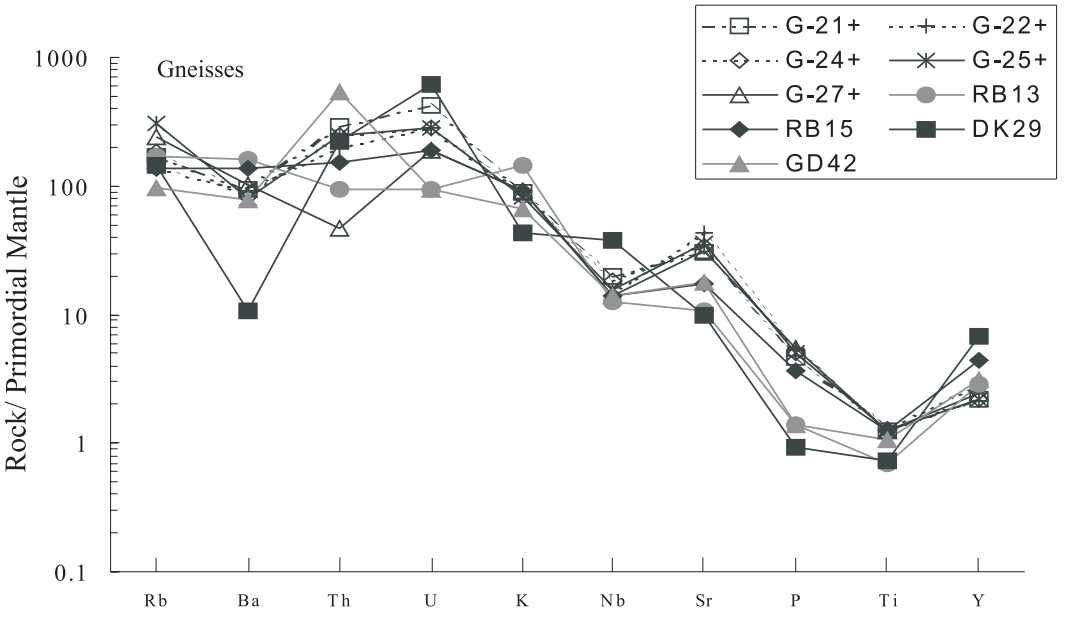

Figure 4**(a)**. Primordial mantle normalized multi-elemental patterns for the gneisses of Bastar and Bundelkhand cratons. Normalizing values are from Sun and McDonough (1989).

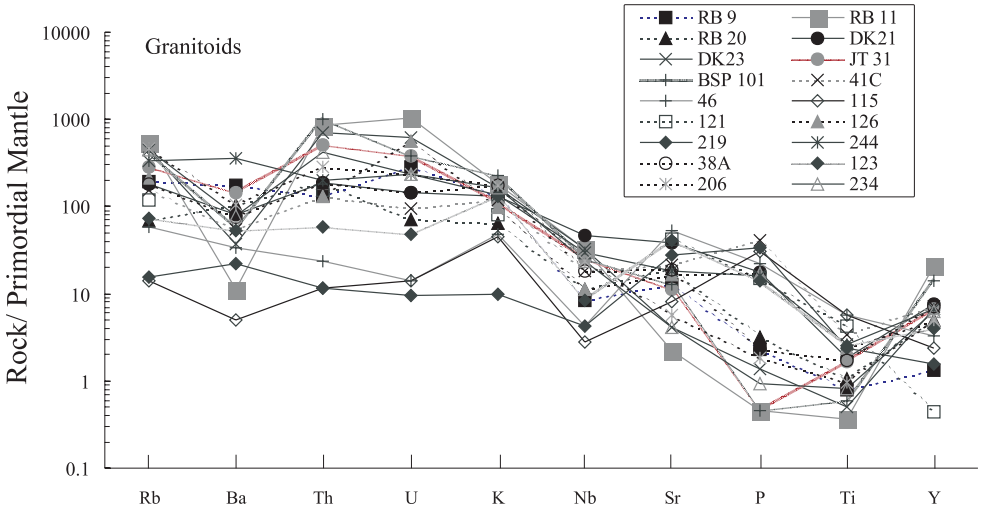

Figure 4**(b)**. Primordial mantle normalized multi-elemental patterns for the granitoids of Bastar and Bundelkhand cratons. Normalizing values are from Sun and McDonough (1989).

zone environment. However, the mode of subduction has remained highly debatable (Martin 1986; Smithies 2000; Moyen *et al* 2003; Smithies *et al* 2003). Some workers believe that TTG are produced by melting of subducted basaltic oceanic crust during Archaean because of the high geothermal gradient (Martin 1986, 1994; Condie 1989; Martin and Moyen 2002; Moyen *et al* 2003). Others opine that TTG are generated by the melting of basaltic material previously either under-plated at the base of a thickened continental crust through magmatic processes (Atherton and Petford 1993; Rudnick 1995) or under-thrusted during flat subduction (Smithies and Champion 2000; Smithies 2000; Smithies *et al* 2003). The main differences among the ideas are based on whether or not the melts derived from the subducted slab interacted with the mantle wedge. Taking into account the elements that are abundant in the mantle wedge and can readily assimilate with the melt from the slab, Martin and Moyen (2002) have observed a secular change in the concentration of these elements

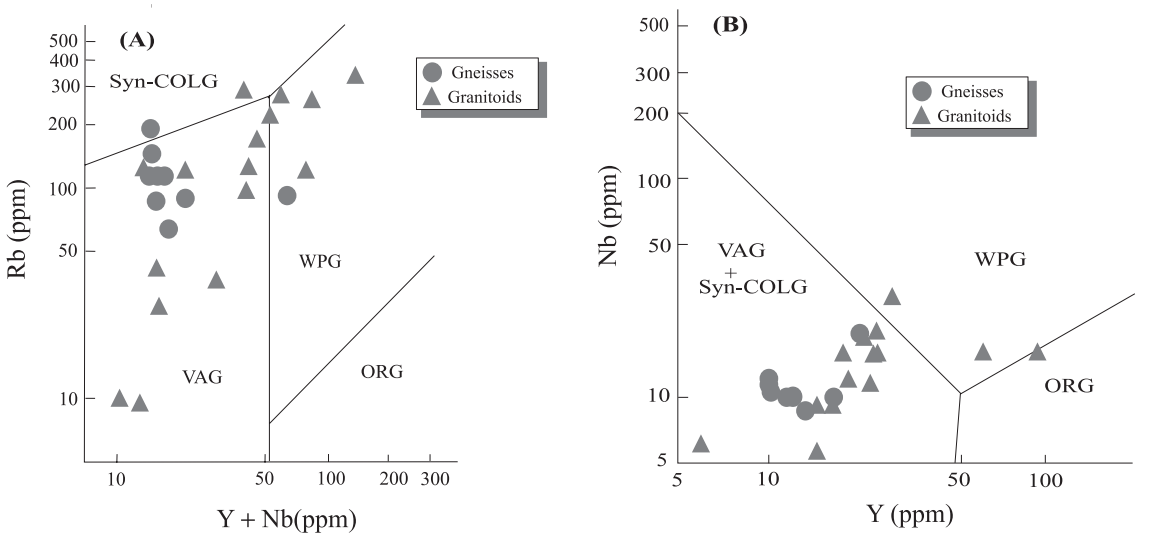

Figure 5. **(A)** Rb vs. Y+Nb and **(B)** Nb vs. Y tectonic discriminant diagram for the gneisses and granitoids of Bastar craton. Fields: **VAG:** volcanic arc granite, **Syn-COLG:** syn-collisional granite, **WPG:** within-plate granite, **ORG:** ocean ridge granite are after Pearce *et al* (1984).

from Archaean to Proterozoic. They have noticed a gradual increase in the Mg# (45 to 65), Sr (550 to 1200 ppm), Ni (30 to 70 ppm) and Cr (50 to 200 ppm) contents over time from early Archaean to Paleo-Proterozoic. They have explained the gradual variation in terms of the gradual decline in geothermal gradient vis-à-vis gradual increase in the depths of melting resulting in increase in melt-mantle interaction. The felsic magmatism of the central Indian Shield complies with such an evolutionary trend. The gneisses of Bundelkhand and Bastar cratons are characterized by average values of Mg#, 33 and 21; Ni, 2 and 10 ppm; Cr 14 and 11 ppm; Sr, 772 and 295 ppm respectively. The corresponding average values of granitoids of Bundelkhand and Bastar cratons are Mg#, 36 and 21; Ni, 49 and 22 ppm; Cr, 49 and 276 ppm; Sr, 452 and 305 ppm.

The low values of Mg#, Cr, Ni and Sr in the gneisses suggest that the precursor slab melts for the gneisses of the central Indian Shield traversed through a very thin mantle wedge minimizing the chances of interaction with it. It is now widely believed that the Archaean oceanic crust was much thicker ($\sim$ 15 to 45 km: Bickle 1986; Abbott *et al* 1994; Ohta *et al* 1996) warmer and buoyant than modern oceanic crust ($\sim$ 7 km) and even thicker than most modern oceanic plateau crust (15–20 km: Gutscher *et al* 2000b). At the present day convergent margins, oceanic plateau crust is obducted or tectonically underplated into the lithosphere rather than getting subducted (Tarney 1992). Thus, a thicker and buoyant Archaean oceanic crust would have resisted subduction (Abbott and Hoffman 1984; Bickle 1986; Abbott *et al* 1994) and if subducted at all it would have subducted at a very low angle. The slab melts from the modern flat subduction (low angle) zones produce rocks with high SiO_2, Na and LILE (called adakites), which are variously defined as an analogue of Archaean TTG. It has been noted that 80% of magmatism from modern flat subductions yield adakites. The geochemical uniformity of the adakites with the Archaean TTG suggests analogous subduction environment during Archaean (Drummond and Defant 1990; Drummond *et al* 1996; Martin 1999). Smithies and Champion (2000) had invoked a low angle subduction (flat subduction) to explain the tectonic framework of the genesis of Archaean TTG suites from Pilbara craton, western Australia. Abbott and Hoffman (1984), Abbott (1991), Tarney and Jones (1994) have also advocated that flat subduction was a significant mode of Archaean subduction that have generated the TTG melts. In this study we also contend that the precursor melts for the gneisses of the central Indian Shield were generated due to melting of a flat subducted oceanic crust and the melts have ascended without interacting the mantle wedge (figure 6).

The slab melts during late Archaean to Paleo-Proterozoic ascended through a peridotite mantle wedge, and this is demonstrated by gradual increase in Mg#, Cr, Ni and decrease in SiO_2 contents (Rapp *et al* 1999). Such high values of Mg#, Cr, Ni and high LILE can be obtained from a subduction modified source also. The huge volume of granitoid magmatism (of batholithic dimension) within the central Indian Shield appears contrary to the subduction-modified source as a thin slice of Archaean mantle wedge metasomatized during earlier cycle(s) of subduction cannot feed such a

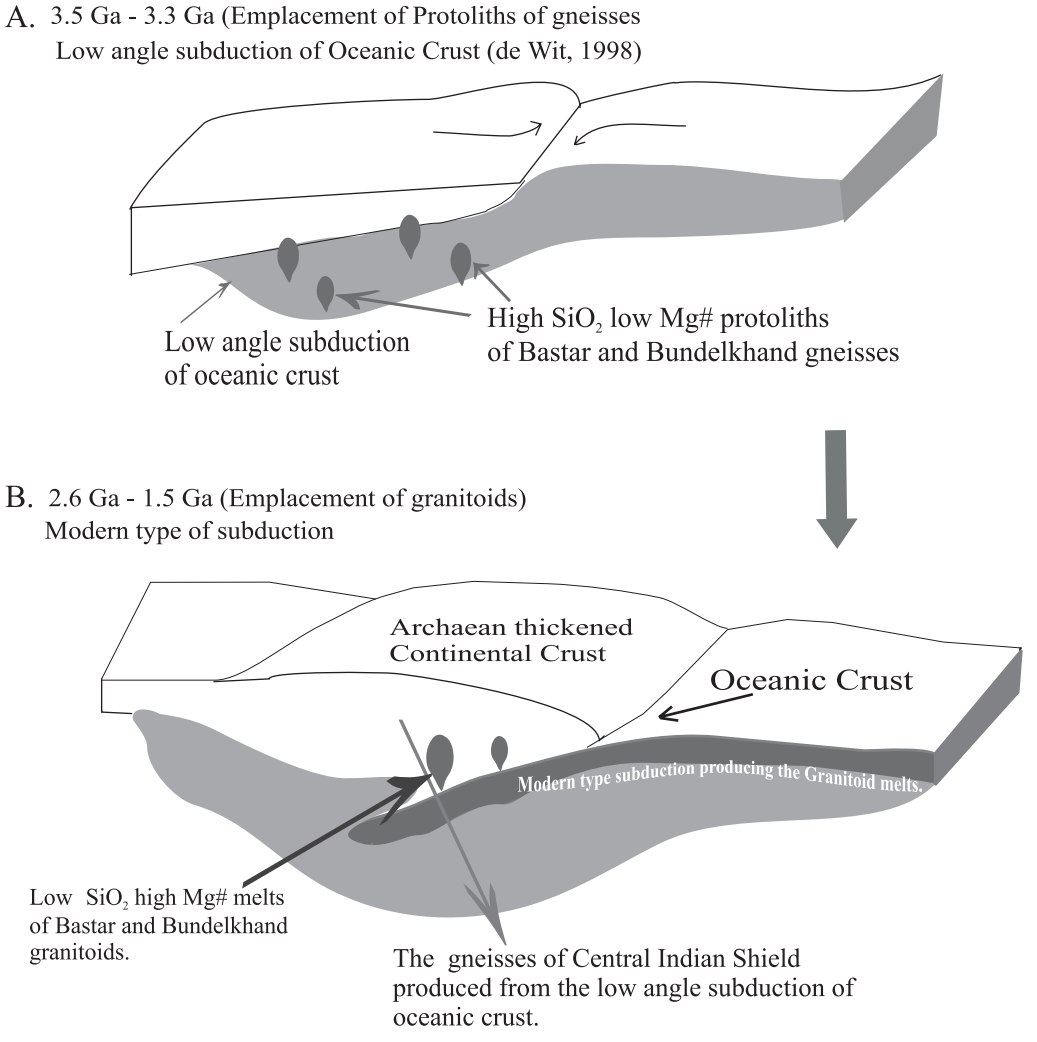

Figure 6. Schematic representation of possible tectonic models for central Indian felsic magmatism.

huge volume of granite magmatism. This demands an independent event of subduction during Proterozoic.

The granitoids of the central Indian Shield have relatively high values of Mg#, Cr, Ni and lower values of SiO_2. To accommodate the observed geochemical characteristics it is proposed that the granitic melts were produced in a high angle subduction environment. The melts generated might have interacted with the mantle wedge (figure 6).

7. Conclusions

It is proposed that the precursor magma for the TTG gneisses of central Indian shield were generated as a result of flat subduction of oceanic crust in the Archaean. The magma thus generated did not interact much with the mantle wedge. In contrast, during late Archaean to Paleo-Proterozoic, the style of subduction changed from flat to high angle and the magma generated traversed through mantle wedge. Thus the granitoids were formed in response to high angle subduction. It can thus be inferred that the tectonic scenario over the central Indian Shield might have changed from a flat low angle subduction during Archaean to a modern type subduction in the Proterozoic. As the subduction ceased, the lithosphere experienced extensional tectonics and as a result mafic dykes were emplaced (Srivastava *et al* 1996). Granitoids emplaced in this tectonic environment have within-plate geochemical signatures. Continued rifting within the Bastar craton led to the development of rift basins and subsequent depositions of younger supracrustals.

Acknowledgements

The authors thank the Directors of WIHG, Dehra-Dun and NGRI, Hyderabad and the Chairman,

Department of Geology, AMU, Aligarh, and Chairman, Department of Geology, University of Delhi, New Delhi for providing facilities to carry out the study. The authors are grateful to Dr. R K Srivastava, BHU, two anonymous reviewers and Dr. H C Sheth, Guest Editor of this special issue for constructive and helpful reviews and suggestions that led to considerable improvements in the final version of the manuscript.

References

Abbott D 1991 The case for accretion of the tectosphere by buoyant subduction; *Geophys. Res. Lett.* **18(4)** 585–588

Abbott D, Drury R and Smith W H F 1994 Flat to steep transition in subduction style; *Geology* **22** 937–940

Abbott D H and Hoffman S E 1984 Archaean plate tectonics revisited, 1. Heat flow, spreading rate and age of subducting oceanic lithosphere and their effects on the origin and the evolution of continents; *Tectonics* **3(4)** 429–448

Acharyya C K and Roy A 2000 Tectonothermal history of the central Indian tectonic zone and reactivation of major faults/shear zones; *J. Geol. Soc. India* **55** 239–256

Atherton M P and Petford N 1993 Generation of sodium-rich magmas from newly underplated basaltic crust; *Nature* **362** 144–146

Ayuso R A and Arth J G 1992 The Northeast Kingdom batholith, Vermont: magmatic evolution and geochemical constraints on the origin of Acadian granitic rocks; *Contrib Miner. Petrol.* **111** 1–23

Barker F and Arth J G 1976 Generation of trondhjemite-tonalitic liquids and Archaean bimodal trondhjemites–basalt suites; *Geology* **4** 596–600

Basu A K 1986 Geology of parts of the Bundelkhand granite massif, central India; *Records Geol. Surv. India* **117** 61–124

Bertrand J M, Duppy C, Dostal J and Davison I 1984 Geochemistry and geotectonic interpretation of granitoids from Central Iforas (Mali, W. Africa); *Precam. Res.* **26** 265–283

Bickle M J 1986 Implication of melting for stabilization of the lithosphere and heat loss in Archaean; *Earth Planet. Sci. Letters* **80** 314–324

Balaram V, Ramesh S L and Anjaiah K V 1996 New trace and REE data in thirteen GSF reference samples by ICP-MS; *Geostandards Newslett.* **20** 71–81

Condie K C 1989 *Plate Tectonics and Crustal Evolution*; 3rd ed. (Pergamon) 476 pp

Drummond M S, Defant M J and Kepezhinskas P K 1996 Petrogenesis of slab derived trondhjemite-tonalite-dacite/adakite magmas; *Trans. Royal Soc. Edinburg* (Earth Sciences) **87** 205–215

Drummond M S and Defant M J 1990 A model for trondhjemite-tonalite-dacite gneisses and crustal growth via slab melting: Archaean to modern comparisons; *J. Geophys. Res.* **95B** 21503–21521

Garrison J M and Davidson J P 2003 Dubious case for slab melting in the Northern Volcanic Zone of the Andes; *Geology* **31** 565–568

Gutscher M-A, Maury R, Eissen J-P and Bourdon E 2000a Can slab melting be caused by flat subduction; *Geology* **28** 535–538

Gutscher M-A, Spakman W, Bijward H and Engdahl E R 2000b Geodynamics of flat subduction: seismicity and tomographic constraints from the Andean margins; *Tectonics* **19** 814–833

Hawkesworth C J, Gallagher K, Hergt J M and McDermott F 1994 Destructive plate margin magmatism: Geochemistry and melt generation; *Lithos* **33** 169–188

Hussain M F, Mondal M E A and Ahmad T 2004 Geochemistry of the basement gneisses and gneissic enclaves from Bastar craton: geodynamic implications; *Curr. Sci.* **86** 1543–1547

Kroner A 1985 Evolution of the Archaean continental crust; *Annual Rev. Earth and Planet. Sci.* **13** 49–74

Martin H 1986 Effect of steeper Archaean geothermal gradient on geochemistry of subduction zone magmas; *Geology* **14** 753–756

Martin H 1987 Petrogenesis of Archaean trondhjemites, tonalites and granodiorites from eastern Finland: Major and trace element geochemistry; *J. Petrol.* **28** 921–953

Martin H 1993 The mechanism of petrogenesis of the Archaean continental crust – comparison with modern processes; *Lithos* **30** 373–388

Martin H 1994 The Archaean grey gneisses and the genesis of continental crust In: *Archaean Crustal Evolution* (ed) K C Condie (Amsterdam: Elsevier) 205–259

Martin H 1999 Adakite Magmas: modern analysis of Archaean granitoids; *Lithos* **46** 411–429

Martin H and Moyen, J F 2002 Secular changes in TTG composition as markers of progressive cooling of the earth; *Geology* **30** 319–322

Mondal M E A 1995 Petrological and geochemical study of the granitic rocks of Bundelkhand Massif in the Jhansi, Lalitpur area, Uttar Pradesh, India; Unpub. Ph.D. Thesis. Aligarh Muslim University, Aligarh, India. 146 pp.

Mondal M E A 2001 Geochemistry and petrogenesis of Proterozoic mafic dykes from Bundelkhand massif, central Indian shield: implications for crustal evolution; *Jour. Applied Geochemistry* **3** 104–119

Mondal M E A and Ahmad T 2001 Bundelkhand mafic dykes, central Indian Shield: implication for the role of sediment subduction in Proterozoic crustal evolution; *Island arc* **10** 51–67

Mondal M E A, Goswami J N, Deomurari M P and Sharma K K 2002 Ion microprobe $^{207}Pb/^{206}Pb$ ages of zircon from the Bundelkhand massif, northern India: implication for crustal evolution of the Bundelkhand–Aravalli protocontinent; *Precamb. Res.* **117** 85–100

Moyen J F, Martin H, Jayananda M and Auvray B 2003 Late Archaean granites: a typology based on the Dharwar craton (India); *Precam. Res.* **127** 103–123

Neogi S, Miura H and Hariya Y 1996 Geochemistry of the Dongargarh volcanic rocks, central India: implications for the Precambrian mantle; *Precam. Res.* **76** 77–91

Ohta H, Maruyama S, Takahasi E, Watanabe Y, and Kato Y 1996 Field occurrence, geochemistry and petrogenesis of the Archaean Mid-Oceanic Ridge basalts (AMORBs) of the Cleaverville area, Pilbara craton, western Australia; *Lithos* **37** 199–221

Peacock S M 1990 Numerical simulation of metamorphic pressure–temperature–time paths and fluid production in subducting slabs; *Tectonics* **9** 1197–1211

Pearce J A, Harris N B W and Tindle A G 1984 Trace element discrimination diagrams for the tectonic interpretations of granitic rocks; *J. Petrol.* **25** 956–983

Radhakrishna B P and Naqvi S M 1986 Precambrian continental crust of India and its evolution; *J. Geol.* **94** 145–166

Rapp P R, Shimizu N, Norman M D and Applegate G S 1999 Reaction between slab derived melts and peridotite

in the mantle wedge: experimental constraints at 3.8 Gpa; *Chem. Geol.* **160** 335–356

Rudnick R L 1995 Making continental crust; *Nature* **378** 571–577

Sarkar A, Sarkar G, Paul D K and Mitra N D 1990 Precambrian geochronology of the Central Indian Shield – A Review; *Geol. Surv. Ind. Spl. Pub.* **28** 453–482

Sarkar A, Trivedi J R, Gopalan K, Singh P N, Das A K, Paul D K 1984 Rb–Sr geochronology of Bundelkhand granitic complex in the Jhansi-Babina-Talbehat sector, U.P., India; *J. Earth Sci. CEISM Seminar* vol. 64–72

Sarkar G, Paul D K, deLaeter J R, McNaughton N J and Mishra V P 1990 A geochemical and Pb, Sr isotopic study of the evolution of granite gneisses from the Bastar craton, Central India; *J. Geol. Soc. India* **35** 480–496

Sarkar G, Corfu F, Paul D K, McNaughton N J, Gupta S N and Bishnui P K 1993 Early Archaean crust in Bastar craton, Central India – a geochemical and isotopic study; *Precamb. Res.* **62** 127–137

Saini N K, Mukherjee P K, Rathi M S, Khanna P P and Purohit K K 1998 A new geochemical reference sample of granite (DG-H) from Dalhousie, Himachal Himalaya; *J. Geol. Soc. India* **52** 603–606

Saunders A D, Norry M J, and Tarney J 1991 Fluid influence on the trace element composition of subduction zone magmas; *Phil. Trans. Royal Soc. London* **335** 377–392

Sharma K K and Rahman A 1995 Occurrences and petrogenesis of Loda Pahar trondhjemitic gneisses from Bundelkhand craton, Central India: Remnant of an early crust; *Curr. Sci.* **69(1)** 613–616

Smithies R H and Champion D C 2000 The Archaean high Mg diorite suite: links to tonalite-trondhjemite-granodiorite magmatism and implications for early Archaean crustal growth; *J. Petrol.* **41** 1653–1671

Smithies R H, Champion D C and Cassidy K F 2003 Formation of earth's early Archaean continental crust; *Precamb. Res.* **127** 89–101

Smithies R H 2000 The Archaean tonalite, trondhjemite granodiorite (TTG) series is not an analogue of Cenozoic adakites; *Earth Planet. Sci. Lett.* **182** 115–125

Srivastava R K, Hall R P, Verma R and Singh R K 1996 Contrasting Precambrian mafic dykes of the Bastar craton, central India: petrological and geochemical characteristics; *J. Geol. Soc. India* **48** 537–546

Sun S S and McDonough W F 1989 Chemical and isotopic systematics of oceanic basalts: implications for mantle composition and processes. In: *Magmatism in the Ocean Basins* (eds) A D Saunders and M J Norry *Geol. Soc. London Spec. Pub. No.* **42** 313–345

Tarney J 1992 Geochemistry and significance of mafic dyke swarms in the Proterozoic. In: *Proterozoic Crustal Evolution* (ed) K C Condie (Amsterdam: Elsevier) 151–179

Tarney J and Jones C E 1994 Trace element geochemistry of orogenic igneous rocks and crustal growth models; *J. Geol. Soc. London* **151** 855–868